Decoherence in a system of strongly coupled quantum oscillators. II. Central-oscillator network

M. A. de Ponte,* M. C. de Oliveira,† and M. H. Y. Moussa‡

Departamento de Física, CCET, Universidade Federal de São Carlos, Via Washington Luiz Km 235, São Carlos, 13565-905, SP, Brazil

(Received 6 January 2004; published 30 August 2004)

In this work we analyze the coherence dynamics and estimate decoherence times of quantum states in a network where a central dissipative oscillator is coupled with $N-1$ peripheral noninteracting dissipative oscillators. The results obtained here are compared with those in part I of this work where a symmetric network was considered. This comparison helps us to understand the influence of the topology of a network on the coherence dynamics of quantum superposition states. As in part I, master equations are derived for regimes of both weak and strong coupling between the oscillators. Decoherence times of particular states of the network are computed and the results are analyzed in the light of state swap and recurrence processes of reduced states of the network. The linear entropies of the joint and reduced systems are also analyzed.

DOI: 10.1103/PhysRevA.70.022325 PACS number(s): 03.67.−a, 03.65.Ud, 03.65.Yz

I. INTRODUCTION

In Part I of this paper, we analyzed the phenomena of nonlocality and decoherence in the context of a network of N interacting dissipative oscillators, assuming a symmetric network where each oscillator interacts with each other. Part II is concerned with the same phenomena, but here we consider a different topology where a central dissipative oscillator is assumed to interact with the remaining $N-1$ noninteracting dissipative oscillators. We refer to this system of interacting oscillators, sketched in Fig. 1, as a central-oscillator network. As in Part I, we analyze, specifically, the decoherence process, focusing here on the central oscillator which, apart from interacting with its respective reservoir, also interacts directly with the remaining $N-1$ noninteracting oscillators. Of course, the central oscillator interacts indirectly with the reservoirs associated with the $N-1$ noninteracting peripheral oscillators which, in their turn, also interact indirectly with each other through oscillator 1. Considering, as we did in Part I, all oscillators to have the same natural frequency ω_0 and all couplings the same strength λ, master equations are derived for both weak and strong coupling regimes. With these master equations, the coherence dynamics of particular states of the network is analyzed, as well as their decoherence times. The results obtained here for the central-oscillator network are compared with those for the symmetric network obtained in Part I of this paper. The comparison shows how the topology of a network affects the coherence dynamics of strongly interacting quantum oscillators.

An important result of Part I was that the lowest normal mode frequency (Ω_ℓ) is given by $\Omega_\ell|_{\min}=\omega_0 N(N-2)/(N-1)^2$, which follows from the coupling strength $\lambda=2\omega_0/(N-1)^2$, and is always larger than zero for $N>2$. We only obtain $\Omega_\ell|_{\min}\approx 0$ in the particular case where $N=2$, where $\lambda=2\omega_0$. Therefore, for a Markovian white noise reservoir we cannot improve the decoherence times of superposition states in a symmetric network with $N>2$. A distinct situation arises in the central-oscillator network, where the minimum of the normal mode Ω_1 is null for any value of N, a situation which follows from $\lambda=2\omega_0/\sqrt{N-1}$. Therefore, even for a Markovian white noise reservoir, the decoherence times of quantum superpositions can be improved in a central-oscillator network. For the case $N=2$, both topologies lead to the same results that were analyzed in Ref. [1]: the decoherence time of a quantum superposition of states ("Schrödinger cat"-like state) $\mathcal{N}_\pm(|\alpha\rangle \pm |-\alpha\rangle)_1$, prepared in oscillator 1, is improved even with Markovian white noise when strong coupling between the oscillators is assumed. Moreover, we demonstrated in Ref. [1] that, when two oscillators with different damping rates $\Gamma_1 \gg \Gamma_2$ are considered, the decoherence time of the superposition $\mathcal{N}_\pm(|\alpha\rangle \pm |-\alpha\rangle)_1$ prepared in oscillator 1 is doubled, even for weak coupling between the oscillators.

As stressed in Part I, over the last few years interest has grown in the coherence dynamics of a quantum network. In

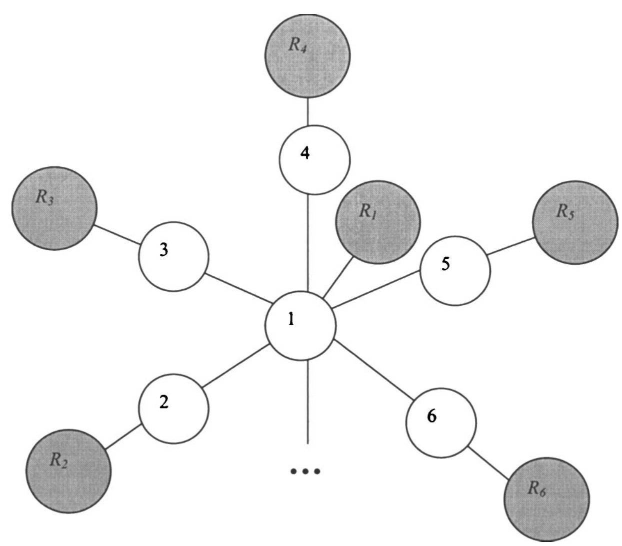

FIG. 1. Sketch of a central-oscillator network where a central dissipative oscillator 1 interacts with $N-1$ peripheral noninteracting dissipative oscillators. Their respective reservoirs are labeled R_m $(m=1,2,\ldots,N)$.

*Electronic address: maponte@df.usfcar.br
†Electronic address: marcos@df.usfcar.br
‡Corresponding author; electronic address: miled@df.usfcar.br

the particular case of a network composed of two oscillators, theoretical models [2,3] and an experimental proposal [4] has been published. As quantum logic operations have been demonstrated experimentally [5–7], it is expected that the investigation of the coherence dynamics in quantum networks proceeds accordingly. In this context, we present here a contribution to the investigation of the effects of the topology on the coherence dynamics of a network of dissipative oscillators.

The current research on coherence dynamics in quantum networks is strongly connected with the program of quantum reservoir engineering [8–11]. In fact, the effect of the strong coupling between the oscillators is essentially to shift the normal-mode frequencies Ω_1 and Ω_ℓ to regions far away from the system natural frequency ω_0. Therefore, the reservoir spectral densities can be explored through the coupling strength between the oscillators and, consequently, the decoherence time can be controlled.

Although investigation of quantum networks has recently been motivated by the interest in quantum computation [12] and communication [13–15], it has attracted attention since long ago. In the 1980s Yurke and Dekker [16] proposed a general approach to analyzing the quantum behavior of complicated electronic circuits which was capable of dealing with electrical networks having nonlinear or dissipative elements. More recently, under the title quantum information theory, Cirac *et al.* [14] presented a scheme to utilize photons for ideal quantum transmission between atoms located at spatially separated nodes of a quantum network. Wang *et al.* [17] have proposed a way of building a universal quantum network that is compatible with the known quantum gate-assembly schemes, easily assembled, reusable, scalable and even potentially programmable. Finally, we note that an effective Hamiltonian to describe charge qubits coupled through a microwave cavity was presented by Zhu *et al.* [18]. The authors show that the ability to interconvert localized charge qubits and flying qubits in the proposed scheme implies that a quantum network can be constructed by scaling up their solid-state system.

Finally, we mention the work by Mahler and Kim [19], a special inhomogeneous quantum network consisting of a ring of M pseudo-spins that were sequentially coupled to one and the same central spin under the influence of given pulse sequences (quantum gate operations). This architecture could be visualized as a quantum Turing machine with a cyclic “tape.” Rather than input-output relations we investigate the resulting process, i.e., the correlation between one- and two-point expectation values (“correlations”) over various time-steps. The resulting spatiotemporal pattern exhibits many nonclassical features including Zeno effects, violation of temporal Bell inequalities and quantum parallelism. Due to the strange web of correlations being built up, specific measurement outcomes for the tape may refer to one or several preparation histories of the head. Specific families of correlation functions are more stable with respect to dissipation than the total wave-function.

II. THE CENTRAL-OSCILLATOR NETWORK

As in the case of a symmetric network (Part I of this paper), we assume here that the interactions between oscillators, as well as between each oscillator and its reservoir, are described by the rotating wave approximation. Moreover, as the strong-coupling limit will be analyzed, a positive-defined Hamiltonian is considered so that the energy spectrum has a lower bound [20,21]. Assuming throughout that the subscript ℓ ranges from 2 to N whereas the subscript n ranges from 1 to N, the system Hamiltonian for the central-oscillator network is given by $(\hbar=1)$

$$H = \sum_\ell \frac{\omega_0}{N-1}\left(a_1^\dagger + (N-1)\frac{\lambda}{2\omega_0}a_\ell^\dagger\right)\left(a_1 + (N-1)\frac{\lambda}{2\omega_0}a_\ell\right) + \sum_\ell \omega_0\left(a_\ell^\dagger + \frac{\lambda}{2\omega_0}a_1^\dagger\right)\left(a_\ell + \frac{\lambda}{2\omega_0}a_1\right) + \sum_{n,k}\omega_{nk}\left(b_{nk}^\dagger + \frac{V_{nk}}{\omega_{nk}}a_n^\dagger\right)\left(b_{nk} + \frac{V_{nk}}{\omega_{nk}}a_n\right), \tag{1}$$

where $a_n^\dagger$ and a_n are, respectively, the creation and annihilation operators for the oscillators, while b_{nk} and $b_{nk}^\dagger$ are the analogous operators for the kth bath oscillator of system n, whose corresponding frequency and coupling strength are written ω_{nk} and V_{nk}, respectively. Assuming that the coupling between the oscillators and their reservoirs satisfies the condition $\Sigma_k (V_{nk})^2/\omega_{nk} \ll \omega_0$ and defining the shifted frequency

$$\tilde{\omega}_0 = \omega_0\left[1 + (N-1)\frac{\lambda^2}{(2\omega_0)^2}\right], \tag{2}$$

we obtain from Eq. (1) the Hamiltonian $H=H_0^S+H_0^R+V$, where

$$H_0^S = \tilde{\omega}_0\sum_n a_n^\dagger a_n + \lambda\sum_\ell (a_1^\dagger a_\ell + a_1 a_\ell^\dagger), \tag{3a}$$

$$H_0^R = \sum_{n,k}\omega_{nk}b_{nk}^\dagger b_{nk}, \tag{3b}$$

$$V = \sum_{n,k} V_{nk}(a_n^\dagger b_{nk} + a_n b_{nk}^\dagger). \tag{3c}$$

As in Part I of this paper, whenever $\lambda/(2\omega_0) \gtrsim 1/\sqrt{N-1}$, the value of $\tilde{\omega}_0$ is significantly shifted away from the natural frequency ω_0 and, in order to ensure an energy spectrum with a lower bound, whatever the value of the coupling strength λ, we have to start from a positive-defined Hamiltonian, given by Eq. (1). The Hamiltonian H_0^S can be diagonalized through the canonical transformation

$$A_1 = \frac{1}{\sqrt{2(N-1)}}\left(-\sqrt{N-1}a_1 + \sum_\ell a_\ell\right), \tag{4a}$$

$$A_j = \frac{1}{\sqrt{(N-j)(N-j+1)}}\left(-(N-j)a_j + \sum_{r=j+1}^{N} a_r\right), \tag{4b}$$

$$A_N = \frac{1}{\sqrt{2(N-1)}}\left(\sqrt{N-1}a_1 + \sum_\ell a_\ell\right), \tag{4c}$$

where, throughout this paper, $j=2,3,\ldots,N-1$ and the operator A_n satisfies the same commutation relation as a_n:

$[A_n,A_m]=0$ and $[A_n,A_m^\dagger]=\delta_{nm}$ $(m=1,\ldots,N)$. These new operators are introduced to decouple the interactions between the central oscillator 1 and the $N-1$ peripheral oscillators, coming from the second term on the right hand side of Eq. (3a). Consequently, indirect interactions between the oscillators will be created through their respective reservoirs, as described by Hamiltonian $\mathbf{H}=\mathbf{H}_0+\mathbf{H}_I$, with

$$\mathbf{H}_0=\sum_n\left(\Omega_n A_n^\dagger A_n+\sum_k\omega_{nk}b_{nk}^\dagger b_{nk}\right), \tag{5a}$$

$$\mathbf{H}_I=\sum_{n,m,k}C_{nm}V_{mk}(A_n^\dagger b_{mk}+A_n b_{mk}^\dagger). \tag{5b}$$

Differently from the case of a symmetric network, where just two different normal modes arise, here we have three different shifted frequencies of the coupled systems

$$\Omega_1=\tilde{\omega}_0-\lambda\sqrt{N-1}, \tag{6a}$$

$$\Omega_j=\tilde{\omega}_0, \tag{6b}$$

$$\Omega_N=\tilde{\omega}_0+\lambda\sqrt{N-1}. \tag{6c}$$

The coefficients C_{nm} appearing in Hamiltonian (5b) satisfy the relations

$$C_{11}=-C_{N1}=-\frac{1}{\sqrt{2}},\quad C_{1\ell}=C_{N\ell}=\frac{1}{\sqrt{2(N-1)}}, \tag{7a}$$

$$C_{j1}=0,\quad C_{jj}=-\sqrt{\frac{N-j}{N-j+1}},\quad C_{jN}=\frac{1}{\sqrt{(N-j+1)(N-j)}}, \tag{7b}$$

$$C_{rj}=\frac{1}{\sqrt{(N-j+1)(N-j)}}\quad\text{for}\quad 1<r<j, \tag{7c}$$

$$C_{rj}=0\quad\text{for}\quad j<r<N. \tag{7d}$$

From here on we follow the same steps as in Part I, to derive the equation for the evolution of the density matrix of the whole system $\rho_{1,\ldots,N}(t)$, in the interaction picture, to the second order of perturbation

$$\frac{d\rho_{1,\ldots,N}(t)}{dt}=-\frac{1}{\hbar^2}\int_0^t dt'\,\mathrm{Tr}_R\boldsymbol{[}\mathbf{V}(t),[\mathbf{V}(t'),\rho_R(0)\otimes\rho(t)]\boldsymbol{]}, \tag{8}$$

where $\mathbf{V}(t)=\exp(i\mathbf{H}_0t/\hbar)\mathbf{H}_I\exp(-i\mathbf{H}_0t/\hbar)$. Defining the reservoir operators $\mathcal{O}_{nm}^\dagger(t)=\Sigma_k V_{mk}b_{mk}^\dagger\exp[i(\omega_{mk}-\Omega_n)]$, so that $\mathbf{V}(t)=\Sigma_{n,m}C_{nm}(A_n^\dagger\mathcal{O}_{nm}+A_n\mathcal{O}_{nm}^\dagger)$, we have to solve the integrals appearing in Eq. (8), related to correlation functions of the form

$$\int_0^t dt'\langle\mathcal{O}_{n'n}(t)\mathcal{O}_{mn}^\dagger(t')\rangle$$
$$=\sum_{k,k'}\int_0^t dt' V_{nk}V_{nk'}\langle b_{nk}b_{nk'}^\dagger\rangle$$
$$\times\exp[-i(\omega_{nk}-\Omega_{n'})t+i(\omega_{nk'}-\Omega_m)t'], \tag{9}$$

where, like n and m, $n'=1,\ldots,N$. Assuming that the reservoir frequencies are very closely spaced to allow a continuum summation and remembering that the function $\mathrm{N}_n(\omega_{nk})$ is defined by

$$\langle b_n^\dagger(\omega_{nk})b_n(\omega_{nk'})\rangle=2\pi\mathrm{N}_n(\omega_{nk})\delta(\omega_{nk}-\omega_{nk'}), \tag{10}$$

then, performing the variable transformations $\tau=t-t'$ and $\varepsilon=\omega_{nk}-\Omega_m$, it follows that

$$\int_0^t dt'\langle\mathcal{O}_{n'n}(t)\mathcal{O}_{mn}^\dagger(t')\rangle$$
$$=\exp[i(\Omega_{n'}-\Omega_m)t]\int_{-\Omega_m}^{\infty}\frac{d\varepsilon}{2\pi}[\sigma_n(\varepsilon+\Omega_m)V_{nk}(\varepsilon+\Omega_m)]^2$$
$$\times[\mathrm{N}_n(\varepsilon+\Omega_m)+1]\int_0^t d\tau e^{-i\varepsilon\tau}. \tag{11}$$

Note that the last integral in Eq. (11) contributes significantly only when $|\varepsilon t|\lesssim 1$, so that the upper limit of the time integration can be extended to infinity. Assuming that $V_{nk}(\varepsilon+\Omega_m)$, $\sigma_n(\varepsilon+\Omega_m)$, and $\mathrm{N}_n(\varepsilon+\Omega_m)$ are functions that vary slowly around the frequency Ω_m (as is usually the case in such derivations), we obtain

$$\int_0^t dt'\langle\mathcal{O}_{n'n}(t)\mathcal{O}_{mn}^\dagger(t')\rangle=\frac{N}{2}\gamma_n(\Omega_m)[\mathrm{N}_n(\Omega_m)+1]$$
$$\times\exp[i(\Omega_{n'}-\Omega_m)t], \tag{12}$$

where the damping rates are defined as

$$\gamma_n(\Omega_m)=\frac{1}{N}V_{nk}^2(\Omega_m)\sigma_n^2(\Omega_m)\int_{-\Omega_{n'}}^{\infty}d\varepsilon\,\delta(\varepsilon). \tag{13}$$

For one of the cases in which we will be interested, where $\Omega_1=0$, $\Omega_j=2\omega_0$, and $\Omega_N=4\omega_0$, we obtain from Eq. (13)

$$\gamma_n(\Omega_1)=\frac{1}{2N}V_{nk}^2(\Omega_1)\sigma_n^2(\Omega_1), \tag{14a}$$

$$\gamma_n(\Omega_\ell)=\frac{1}{N}V_{nk}^2(\Omega_\ell)\sigma_n^2(\Omega_\ell). \tag{14b}$$

In the weak coupling regime, defining $\Gamma_n=V_{nk}^2(\omega_0)\sigma_n^2(\omega_0)$, we obtain from Eq. (13) the result

$$\gamma_n(\Omega_m)=\frac{1}{N}V_{nk}^2(\omega_0)\sigma_n^2(\omega_0)=\frac{\Gamma_n}{N}. \tag{15}$$

We note that the minimum of the normal mode Ω_1 is null, $\Omega_1|_{\min}=0$, a value which follows from $\lambda=2\omega_0/\sqrt{N-1}$. In the particular case where $N=2$, we obtain the minimum $\Omega_1|_{\min}$

$=0$ with $\lambda=2\omega_0$, as discussed in Ref. [1]. In what follows, considering the general case of N coupled oscillators, we will be interested in two different coupling strengths: $\lambda=2\omega_0/\sqrt{N-1}$, so that $\Omega_1=0$, $\Omega_j=2\omega_0$, and $\Omega_N=4\omega_0$, and, to compare with the results for a symmetric network, we also consider $\lambda=2\omega_0$, where $\Omega_1=\omega_0(N-2\sqrt{N-1})$, $\Omega_j=N\omega_0$, and $\Omega_N=\omega_0(N+2\sqrt{N-1})$.

We finally note that the assumption that V_n, σ_n, and N_n are functions that vary slowly around the frequency Ω_m does not apply to the function $\mathrm{N}_n(\Omega_1)=[\exp(\hbar\Omega_1/kT)-1]^{-1}$ when considering, in the strong-coupling limit, the reservoir to be in thermal equilibrium at temperature T and the coupling strength $\lambda=2\omega_0/\sqrt{N-1}$, since in this case $\Omega_1\approx 0$. However, this assumption can safely be applied to a reservoir at absolute zero, the situation we analyze in this paper. In practice, $\mathrm{N}_n(\Omega_1)\approx 0$ whenever the shifted frequency Ω_1, arising from the contribution of the Cauchy principal value, becomes sufficiently greater than kT.

III. THE MASTER EQUATION

Defining, in the strong-coupling regime, the simplified expressions $\gamma_n(\Omega_1)=\gamma_n^-$, $\gamma_n(\Omega_j)=\gamma_n$, and $\gamma_n(\Omega_N)=\gamma_n^+$, as well as $\mathrm{N}_n(\Omega_1)=\mathrm{N}_n^-$, $\mathrm{N}_n(\Omega_j)=\mathrm{N}_n$, and $\mathrm{N}_n(\Omega_N)=\mathrm{N}_n^+$ [which reduce to $\gamma_n^-=\gamma_n=\gamma_n^+=\Gamma_n/N$ and $\mathrm{N}_n^-=\mathrm{N}_n=\mathrm{N}_n^+=\mathrm{N}_n(\omega_0)$ in the weak-coupling regime], and using Eqs. (4a)–(4c) along with the coefficients C_{mn} defined above, we obtain the master equation in the Schrödinger picture

$$\frac{d\rho_{1,\ldots,N}(t)}{dt}=i\left[\rho_{1,\ldots,N}(t),\tilde{\omega}_0\sum_n a_n^\dagger a_n+\lambda\sum_\ell\,(a_\ell^\dagger a_1+a_\ell a_1^\dagger)\right]+\sum_n\mathcal{L}_n\rho_{1,\ldots,N}(t)+\sum_{\ell,n(n\neq\ell)}\mathcal{L}_{\ell n}\rho_{1,\ldots,N}(t), \quad (16)$$

where the Liouville operators $\mathcal{L}_n\rho_S(t)$ are given by

$$\mathcal{L}_1\rho_{1,\ldots,N}(t)=\frac{N}{4}(\gamma_1^-+\gamma_1^+)([a_1\rho_{1,\ldots,N}(t),a_1^\dagger]+[a_1,\rho_{1,\ldots,N}(t)a_1^\dagger])+\frac{N}{4}(\gamma_1^+\mathrm{N}_1^++\gamma_1^-\mathrm{N}_1^-)([[a_1,\rho_{1,\ldots,N}(t)],a_1^\dagger]+[a_1,[\rho_{1,\ldots,N}(t),a_1^\dagger]]), \quad (17a)$$

$$\mathcal{L}_\ell\rho_{1,\ldots,N}(t)=N\frac{\gamma_\ell^++2(N-2)\gamma_\ell+\gamma_\ell^-}{4(N-1)}([a_\ell\rho_{1,\ldots,N}(t),a_\ell^\dagger]+[a_\ell,\rho_{1,\ldots,N}(t)a_\ell^\dagger])+N\frac{\gamma_\ell^+\mathrm{N}_\ell^++2(N-2)\gamma_\ell N_\ell+\gamma_\ell^-\mathrm{N}_\ell^-}{4(N-1)}\times([[a_\ell,\rho_{1,\ldots,N}(t)],a_\ell^\dagger]+[a_\ell,[\rho_{1,\ldots,N}(t),a_\ell^\dagger]]), \quad (17b)$$

whereas the cross-decay channels are here separated into direct-cross-decay channels and indirect-cross-decay channels, which are given, respectively, by

$$\mathcal{L}_{\ell 1}\rho_{1,\ldots,N}(t)=\frac{N}{4\sqrt{N-1}}\{(\gamma_1^+-\gamma_1^-)([a_\ell\rho_{1,\ldots,N}(t),a_1^\dagger]+[a_1,\rho_{1,\ldots,N}(t)a_\ell^\dagger])+(\gamma_1^+\mathrm{N}_1^+-\gamma_1^-\mathrm{N}_1^-)\times([[a_\ell,\rho_{1,\ldots,N}(t)],a_1^\dagger]+[a_1,[\rho_{1,\ldots,N}(t),a_\ell^\dagger]])+(\gamma_\ell^+-\gamma_\ell^-)([a_\ell,\rho_{1,\ldots,N}(t)a_1^\dagger]+[a_1\rho_{1,\ldots,N}(t),a_\ell^\dagger])+(\gamma_\ell^+\mathrm{N}_\ell^+-\gamma_\ell^-\mathrm{N}_\ell^-)\times([a_\ell,[\rho_{1,\ldots,N}(t),a_1^\dagger]]+[[a_1,\rho_{1,\ldots,N}(t)],a_\ell^\dagger])\}, \quad (18a)$$

$$\mathcal{L}_{\ell\ell'}\rho_{1,\ldots,N}(t)=\frac{N}{4(N-1)}\{(\gamma_{\ell'}^--2\gamma_{\ell'}+\gamma_{\ell'}^+)([a_\ell\rho_{1,\ldots,N}(t),a_{\ell'}^\dagger]+[a_{\ell'},\rho_{1,\ldots,N}(t)a_\ell^\dagger])+(\gamma_{\ell'}^+\mathrm{N}_{\ell'}^+-2\gamma_{\ell'}\mathrm{N}_{\ell'}+\gamma_{\ell'}^-\mathrm{N}_{\ell'}^-)\times([[a_\ell,\rho_{1,\ldots,N}(t)],a_{\ell'}^\dagger]+[a_{\ell'},[\rho_{1,\ldots,N}(t),a_\ell^\dagger]])\}. \quad (18b)$$

The master equation (16) is a general form valid for the strong coupling regime. Evidently, the cross-decay channels $\mathcal{L}_{\ell n}\rho_S(t)$, owing to the strong coupling between the systems, can be of the same order of magnitude as the direct-decay channels $\mathcal{L}_n\rho_S(t)$. In the weak coupling regime, where $\gamma_n^-=\gamma_n=\gamma_n^+=\Gamma_n/N$ and $\mathrm{N}_n^-=\mathrm{N}_n=\mathrm{N}_n^+=\mathrm{N}_n(\omega_0)$ (see discussion below), the cross-decay channels cancel out and the master equation (16) reduces to the expected form for N independent dissipative oscillators where the Liouville operators simplify to the well-known structure

$$\mathcal{L}_n'\rho_{1,\ldots,N}(t)=\tfrac{1}{2}\Gamma_n\{([a_n\rho_{1,\ldots,N}(t),a_n^\dagger]+[a_n,\rho_{1,\ldots,N}(t)a_n^\dagger])+N_n(\omega_0)([[a_n,\rho_{1,\ldots,N}(t)],a_n^\dagger]+[[a_n^\dagger,\rho_{1,\ldots,N}(t)],a_n])\}. \quad (19)$$

It is important to stress that for a network with a large number of oscillators, all the normal modes can be shifted to regions far away from the natural frequency ω_0 even for small values of the coupling strength λ. As observed in Part I, this is a crucial feature of a network with $N\gg 1$, since in this case we have always to consider the cross-decay channels, emerging from differing values for the damping rates γ_n^-, γ_n, and γ_n^+. In a realistic quantum logical processor, the number of dissipative nodes must always be taken into account—when analyzing the coherence dynamics and decoherence times—even in the case of weak coupling between these nodes.

A. The split in the damping rates and spectral densities of the reservoirs

As remarked in Part I of this work, among other aspects of strongly coupled systems, we explore the applications of the splitting of the damping rates of the oscillators that arise from the split in the natural frequency ω_0 into the normal modes of the network. To illustrate the mechanism of the split in the damping rates, which leads to the cross-decay channels, we assume, as in Part I, a Lorentzian coupling V_ℓ between the oscillators and their respective reservoirs. The damping function $\Gamma_n(\chi)$ thus displays a Lorentzian shape, centered around ω_0 in the weak-coupling regime, such that

$$\Gamma_n(\chi) = \sigma_n^2 \frac{\varkappa}{(\chi-\omega_0)^2+\varkappa^2}, \tag{20}$$

where the parameter $\varkappa$ represents the spectral sharpness around the mode frequency. In the strong-coupling regime the above damping function splits (owing to the split in the natural frequency ω_0 into three distinct normal modes Ω_1, Ω_j, and Ω_N) into three Lorentzian functions:

$$\Gamma_n(\chi) = \frac{\varkappa\sigma_n^2}{N}\left(\frac{1}{(\chi-\Omega_1)^2+\varkappa^2} + \sum_j \frac{1}{(\chi-\Omega_j)^2+\varkappa^2} + \frac{1}{(\chi-\Omega_N)^2+\varkappa^2}\right)$$
$$= \gamma_n(\Omega_1) + \sum_j \gamma_n(\Omega_j) + \gamma_n(\Omega_N). \tag{21}$$

In the weak-coupling regime, where $\Omega_n \approx \omega_0$, we obtain from Eqs. (15) and (21) that $\gamma_n(\omega_0)+\Sigma_j\gamma_n(\omega_0)+\gamma_n(\omega_0)=\Gamma_m$ and the general Liouville operators in Eqs. (17a) and (17b) reduce to the usual Liouville form for N independent dissipative oscillators (19). In this regime, the damping rate, assumed to be the maximum of a sharp-peaked damping function, i.e., $\Gamma_m(\omega_0)=\Gamma_m$ (for a small value of $\varkappa$), becomes N times higher than the value designated for $\gamma_n(\Omega_1)$, $\gamma_n(\Omega_j)$, and $\gamma_n(\Omega_N)$, individually.

The splitting of the Lorentzian in Eq. (20) into those in Eq. (21) becomes more pronounced as λ and/or N increase. As explained above, a large number of oscillators in the network also shift the normal modes to regions far away from the natural frequency ω_0. As a consequence, the spectral densities of the reservoirs can be employed to control the decoherence of quantum states of the network, if the normal modes are shifted to regions of the frequency space with spectral density significantly smaller than that around ω_0. In other words, we have to increase the parameter $\lambda\sqrt{N-1}$, by raising the coupling strength and/or the number of oscillators in the network, to enable us to explore regions of frequency space different from that around ω_0. In this light, from here on we use the term "strong-coupling regime" to describe situations where the parameter $\lambda\sqrt{N-1}$ is large enough for the cross-decay channels to have to be taken into account.

Instead of analyzing various spectral densities of the reservoir, to illustrate the interesting features arising from the strong-coupling regime, we next consider only a Markovian white noise reservoir. A more detailed discussion can be found in Part I. As the spectral density of a Markovian white noise reservoir is invariant over translation in frequency space, if we assume a Lorentzian coupling between the oscillators and their respective reservoirs—centered around the normal-mode frequencies, as in Eq. (21)—we get from Eq. (13) the results $\gamma_m^- = \Gamma_m/2N$ and $\gamma_m = \gamma_m^+ = \Gamma_m/N$ (following from the coupling strength $\lambda = 2\omega_0/\sqrt{N-1}$). Therefore, the damping rate around $\Omega_1 \approx 0$ has half the value around the normal modes Ω_j and Ω_N. After deriving the Fokker–Planck equation and estimating the decoherence times of quantum states of the network, the effect of the damping rate γ_m^- will be analyzed and the decoherence times in different topologies will be compared.

IV. THE FOKKER–PLANCK EQUATION

From the master equation (16), we derive the Fokker–Planck equation for the P-representation:

$$\frac{d}{dt}P(\{\eta_n\},t) = \sum_m \left(\Pi_m + C_m(\{\eta_n\})\frac{\partial}{\partial\,\eta_m} + \sum_n D_{mn}\frac{\partial^2}{\partial\,\eta_m\,\partial\,\eta_n^*} + \text{c.c.}\right)P(\{\eta_n\},t), \tag{22}$$

where the function $C_m(\{\eta_n\})$ and the matrix elements D_{mn} satisfy

$$C_1(\{\eta_n\}) = (A_1 + i\tilde{\omega}_0)\eta_1 + B_1\sum_\ell \eta_\ell, \tag{23a}$$

$$C_\ell(\{\eta_n\}) = B_\ell\eta_1 + \left(\frac{N}{2}\gamma_\ell + i\tilde{\omega}_0\right)\eta_\ell + A_\ell\sum_{\ell'}\eta_{\ell'}, \tag{23b}$$

$$D_{11} = \frac{N}{4}(\gamma_1^+ \mathrm{N}_1^+ + \gamma_1^- \mathrm{N}_1^-), \tag{23c}$$

$$D_{1\ell} = D_{\ell 1} = \frac{N}{8\sqrt{N-1}}(\gamma_1^+\mathrm{N}_1^+ + \gamma_\ell^+\mathrm{N}_\ell^+ - \gamma_1^-\mathrm{N}_1^- - \gamma_\ell^-\mathrm{N}_\ell^-), \tag{23d}$$

$$D_{\ell\ell'} = \frac{N}{4(N-1)}\{\gamma_\ell^+\mathrm{N}_\ell^+ + 2[(N-1)\delta_{\ell\ell'} - 1]\gamma_\ell\mathrm{N}_\ell + \gamma_\ell^-\mathrm{N}_\ell^-\}, \tag{23e}$$

while the parameters Π_m, A_m, and B_m are given by

$$\Pi_1 = \frac{N}{4}(\gamma_1^- + \gamma_1^+), \tag{24a}$$

$$\Pi_\ell = \frac{N}{4(N-1)}[\gamma_\ell^+ + 2(N-2)\gamma_\ell + \gamma_\ell^-], \tag{24b}$$

$$A_1 = \frac{N}{4}(\gamma_1^- + \gamma_1^+), \tag{24c}$$

$$A_\ell = \frac{N}{4(N-1)}(\gamma_\ell^- - 2\gamma_\ell + \gamma_\ell^+), \tag{24d}$$

$$B_n = \frac{N}{4\sqrt{N-1}}(\gamma_n^+ - \gamma_n^-) + i\lambda. \tag{24e}$$

For a reservoir at absolute zero, the Fokker–Planck (FP) equation (22) reduces to the drift equation

$$\frac{d}{dt}P(\{\eta_n\},t) = \sum_m \left(\Pi_m + C_m(\{\eta_n\})\frac{\partial}{\partial \eta_m} + \text{c.c.}\right)P(\{\eta_n\},t), \tag{25}$$

and following the procedure used to solve the equivalent drift equation for the symmetric network (in part I), we apply the transformation $P(\{\eta_n\},t)=\widetilde{P}(\{\eta_n\},t)\exp(2\Sigma_m\Pi_m t)$ and assume a solution of Eq. (25) of the form $\widetilde{P}(\{\eta_n\},t)=\widetilde{P}(\{\eta_n(t)\})$, obtaining

$$\frac{d\widetilde{P}}{dt} = \sum_m \left(\frac{d\eta_m}{dt}\frac{\partial \widetilde{P}}{\partial \eta_m} + \text{c.c.}\right) = \sum_m \left(C_m(\{\eta_n\})\frac{\partial \widetilde{P}}{\partial \eta_m} + \text{c.c.}\right). \tag{26}$$

To find an analytical solution to the following system [which results from Eq. (26)]

$$\frac{d\eta_1}{dt} = (A_1 + i\widetilde{\omega}_0)\eta_1 + B_1\sum_\ell \eta_\ell, \tag{27a}$$

$$\frac{d\eta_\ell}{dt} = B_\ell\eta_1 + \left(\frac{N}{2}\gamma_\ell + i\widetilde{\omega}_0\right)\eta_\ell + A_\ell\sum_{\ell'} \eta_{\ell'}, \tag{27b}$$

we assume that all the oscillators of the network have the same damping rate $\Gamma_m=\Gamma$, so that $\gamma_m^\pm=\gamma^\pm$ and $\gamma_m=\gamma$. In this case, the solution of Eqs. (27a) and (27b) is given by $\eta_m(t)=e^{i\widetilde{\omega}_0 t}\Sigma_n\chi_{mn}(t)\eta_n^0$, where $\eta_n^0=\eta_m(t=0)$ and

$$\chi_{11}(t) = f_1(t)g_1(t) + if_2(t)g_2(t), \tag{28a}$$

$$\chi_{1\ell}(t) = \chi_{\ell 1}(t) = \frac{1}{\sqrt{N-1}}[f_1(t)g_2(t) + if_2(t)g_1(t)], \tag{28b}$$

$$\chi_{\ell\ell'}(t) = \frac{1}{N-1}\left[f_1(t)g_1(t) + if_2(t)g_2(t) - \exp\left(\frac{N}{2}\gamma t\right)\right] + \delta_{\ell\ell'}\exp\left(\frac{N}{2}\gamma t\right), \tag{28c}$$

where, like ℓ, $\ell'=2,\ldots,N$. The time-dependent functions appearing in Eqs. (28a)–(28c) are given by

$$f_1(t) = \cos(\lambda\sqrt{N-1}t), f_2(t) = \sin(\lambda\sqrt{N-1}t), \tag{29a}$$

$$g_1(t) = \frac{1}{2}\left[\exp\left(\frac{N}{2}\gamma^+ t\right) + \exp\left(\frac{N}{2}\gamma^- t\right)\right], \tag{29b}$$

$$g_2(t) = \frac{1}{2}\left[\exp\left(\frac{N}{2}\gamma^+ t\right) - \exp\left(\frac{N}{2}\gamma^- t\right)\right]. \tag{29c}$$

Finally, the solution of the drift equation (25) reads

$$P(\{\eta_n\},t) = e^{2[\Pi_1+(N-1)\Pi_2]t}P(\{\eta_n\},t=0)_{\eta_\ell\to\eta_\ell(t)}. \tag{30}$$

V. THE DENSITY OPERATOR

In this section we obtain (for the case $\Gamma_m=\Gamma$) the density operator $\rho_{1,\ldots,N}(t)$ by supposing that the N oscillators are prepared in a superposition of coherent states of the form

$$|\Psi_{1,\ldots,N}\rangle = \mathcal{N}(e^{i\delta_1}|\{\beta_m^1\}\rangle + e^{i\delta_2}|\{\beta_m^2\}\rangle + \cdots + e^{i\delta_J}|\{\beta_m^J\}\rangle) \equiv \mathcal{N}\sum_{p=1}^{J} e^{i\delta_p}|\{\beta_m^p\}\rangle, \tag{31}$$

where $\mathcal{N}$ stands for the normalization factor, δ_p indicates a phase associated with each state in the superposition, and the subscripts (superscripts) label the N oscillators (J distinct states in the superposition). The density operator for the state (31) is written as

$$\rho_{1,\ldots,N}(t) = \int P(\{\eta_n\},t)|\{\eta_n\}\rangle\langle\{\eta_n\}|d^2\{\eta_n\} = \mathcal{N}^2\sum_{p,q=1}^{J} e^{\phi_{pq}+i(\delta_p+\delta_q)}\prod_m \langle\beta_m^q|\beta_m^p\rangle^{1-\Upsilon_{mm}}|\xi_m^p\rangle\langle\xi_m^q|, \tag{32}$$

where, assuming henceforth that $p,q=1,2,\ldots,J$, the phase ϕ_{pq} is given by

$$\phi_{pq} = \frac{1}{2}\sum_{m,n(m\neq n)}[\beta_m^p(\beta_n^{*p} - \beta_n^{*q}) - \beta_n^{q*}(\beta_m^p - \beta_m^q)]\Upsilon_{nm}, \tag{33}$$

while the evolved states of the oscillators satisfy

$$\xi_m^p(t) = \sum_n \mu_{mn}(t)\beta_n^p, \tag{34}$$

with

$$\Upsilon_{mn}(t) = \sum_{n'} \mu_{n'm}^*(t)\mu_{n'n}(t), \tag{35a}$$

$$\mu_{mn}(t) = e^{-i\widetilde{\omega}_0 t}\chi_{mn}(-t). \tag{35b}$$

Finally, the reduced density operator for the mth oscillator, obtained by removing the degrees of freedom of all the remaining oscillators, i.e., $\rho_m(t)=\mathrm{Tr}_{n\neq m}\rho_{1,\ldots,N}$, is given by

$$\rho_m(t) = \mathcal{N}^2\sum_{p,q} e^{\theta_m^{pq}(t)+i(\delta_p+\delta_q)}\left(\prod_n \langle\beta_n^q|\,\beta_n^p\rangle^{1-|\mu_{mn}(t)|^2}\right)|\xi_m^p\rangle\langle\xi_m^q|, \tag{36}$$

where

$$\theta_m^{pq}(t) = \frac{1}{2}\sum_{n,n'(n\neq n')}[\beta_n^p(\beta_{n'}^{*p} - \beta_{n'}^{*q}) - \beta_{n'}^{q*}(\beta_n^p - \beta_n^q)]\mu_{mn'}^*(t)\mu_{mn}(t). \tag{37}$$

From Eq. (36) we can obtain the density matrix for the central oscillator, $\rho_1(t)$, and also for any other oscillator, ℓ, coupled to the central one, i.e., $\rho_\ell(t)$.

VI. DECOHERENCE TIMES

For a central-oscillator network we proceed to estimate the decoherence times for some particular states of the network, remembering that we are considering the case where all the oscillators in the network have the same damping factor $\Gamma_m=\Gamma$. For technical reasons we do not analyze here the case where the damping factor Γ_1 of the central oscillator 1 differs from the others which are all assumed to be the same: $\Gamma_\ell=\Gamma_2$. However, this case, where Γ_1 differs from $\Gamma_\ell=\Gamma_2$, leads exactly to the results obtained for a symmetric network (analyzed in Part I of the present paper) for the weak-coupling regime, when the cross-decay channels become null. Therefore, in this case we lose the results concerned with the strong-coupling regime.

Noting that in the central-oscillator network there is a symmetry between the $N-1$ oscillators $(2,\ldots,N)$ coupled to the central one, we estimate the decoherence time for the superposition state which is a particular case of the state (31):

$$|\psi_{1,\ldots,N}\rangle=\mathcal{N}\Bigg(\Bigg|\alpha,\underbrace{\alpha,\ldots,\alpha}_{R},\underbrace{-\alpha,\ldots,-\alpha}_{S},\underbrace{\eta,\ldots,\eta}_{N-R-S-1}\Bigg\rangle \pm\Bigg|-\alpha,\underbrace{-\alpha,\ldots,-\alpha}_{R},\underbrace{\alpha,\ldots,\alpha}_{S},\underbrace{\eta,\ldots,\eta}_{N-R-S-1}\Bigg\rangle\Bigg) \tag{38}$$

where the first coherent state in both kets refers to the central oscillator (1)1. R (S) indicates the number of the remaining oscillators in the coherent state α $(-\alpha)$, in the first term of the superposition, and $-\alpha(\alpha)$ in the second term of the superposition. The remaining $N-R-S-1$ oscillators are in the coherent state η. The symmetry among the $N-1$ peripheral oscillators makes them indistinguishable. Therefore, swapping the states of any two oscillators, ℓ and ℓ', coupled to the central oscillator 1, we obtain a state which is completely equivalent to Eq. (38). We also note that when $R=S=0$, we obtain from (38) the superposition

$$|\tilde{\psi}_{1,\ldots,N}\rangle=\mathcal{N}_\pm(|\alpha\rangle\pm|-\alpha\rangle)_1\otimes|\{\eta_\ell\}\rangle, \tag{39}$$

where a "Schrödinger cat"-like state is prepared in oscillator 1 while all the other oscillators ℓ are prepared in the coherent states η.

The density operator of the state $|\psi_{1,\ldots,N}\rangle$, derived from Eq. (32), is given by

$$\rho_{1,\ldots,N}(t)=\mathcal{N}^2\sum_{p,q=1}^{2}(\pm)^{1-\delta_{pq}}\exp\{-2|\alpha|^2[1-\Upsilon_{11}+(1+\Upsilon_{\ell\ell'(\ell\neq\ell')}-\Upsilon_{\ell\ell})(R+S)-2(R-S)\Upsilon_{1\ell}-(R-S)^2\Upsilon_{\ell\ell'(\ell\neq\ell')}](1-\delta_{pq})+\phi_{pq}\}|\{\xi_m^p\}\rangle\langle\{\xi_m^q\}|, \tag{40}$$

where, as follows from Eq. (33),

$$\phi_{pq}=2i(N-R-S-1)\mathrm{Im}\left[\eta\left(\Upsilon_{1\ell}\beta_1^{*p}+\Upsilon_{\ell\ell'(\ell\neq\ell')}\sum_{j=2}^{1+R+S}\beta_j^{*p}\right)\right], \tag{41}$$

and from Eq. (35a)

$$\Upsilon_{11}=\tfrac{1}{2}[\exp(-N\gamma^-t)+\exp(-N\gamma^+t)], \tag{42a}$$

$$\Upsilon_{1\ell}=\frac{1}{2\sqrt{N-1}}[\exp(-N\gamma^+t)-\exp(-N\gamma^-t)], \tag{42b}$$

$$\Upsilon_{\ell\ell'}=\frac{1}{2(N-1)}\{\exp(-N\gamma^-t)+\exp(-N\gamma^+t)+2[(N-1)\delta_{\ell\ell'}-1]\exp(-N\gamma t)\}. \tag{42c}$$

The coherence decay of the superposition state (38), computed from Eq. (40), is described by the expression

$$\exp\left\{-2|\alpha|^2\left[1-\frac{1}{2}\left(1+\frac{(R-S)^2}{N-1}\right)[\exp(-N\gamma^-t)+\exp(-N\gamma^+t)]-(R-S)\frac{\sqrt{N-1}}{N-1}[\exp(-N\gamma^+t)-\exp(-N\gamma^-t)]+[1-\exp(-N\gamma t)](R+S)+\exp(-N\gamma t)\frac{(R-S)^2}{(N-1)}\right]\right\}, \tag{43}$$

and so the decoherence time obeys

$$\tau_D/|_{|\psi_{1,\ldots,N}\rangle}=\frac{(N-1)}{N|\alpha|^2}\{[(R-S)^2+N-1](\gamma^-+\gamma^+)-2(R-S)\times\sqrt{N-1}(\gamma^--\gamma^+)+2\gamma[(N-1)(R+S)-(R-S)^2]\}^{-1}. \tag{44}$$

When $R=N-1$ $(S=0)$, leading to the superposition $|\phi_{1,\ldots,N}\rangle=\mathcal{N}(|\alpha_1,\ldots,\alpha_N\rangle\pm|-\alpha_1,\ldots,-\alpha_N\rangle)$ (where $\alpha_m=\alpha$), we get the result

$$\tau_D/|_{|\phi_{1,\ldots,N}\rangle}=\frac{1}{|\alpha|^2N[N(\gamma^++\gamma^-)+2\sqrt{N-1}(\gamma^+-\gamma^-)]}. \tag{45}$$

Although $|\phi_{1,\ldots,N}\rangle$ is an eigenstate of normal mode Ω_1 for the symmetric network, it is not the eigenstate of any normal mode for the central-oscillator network. We note that for $N=1$ and, consequently, $\gamma^+=\gamma^-=\Gamma$, we obtain the expected result for the decoherence of the superposition state $\mathcal{N}_\pm(|\alpha\rangle\pm|-\alpha\rangle)$, given by $(2|\alpha|^2\Gamma)^{-1}$. On the other hand, when $R=S-1$, corresponding to a family of superposition states (which are eigenstates of normal mode Ω_ℓ for the symmetric network but are not eigenstates of the central-oscillator network),

$$\widetilde{\phi}_{1,\ldots,N} = \mathcal{N}\Big(\Big|\underbrace{\alpha,\ldots,\alpha}_{S},\underbrace{-\alpha,\ldots,-\alpha}_{S},\underbrace{\eta,\ldots,\eta}_{N-2S}\Big\rangle \pm \Big|\underbrace{-\alpha,\ldots,-\alpha}_{S},\underbrace{\alpha,\ldots,\alpha}_{S},\underbrace{\eta,\ldots,\eta}_{N-2S}\Big\rangle\Big)$$

we obtain the result

$$\tau_D|_{|\tilde{\phi}_{1,\ldots,N}} = \frac{N-1}{|\alpha|^2 N[N(\gamma^- + \gamma^+ - 2\gamma) + 2\sqrt{N-1}(\gamma^- - \gamma^+) + 4S(N-1)\gamma]}. \tag{46}$$

Finally, when $R=S=0$, leading to the state $|\tilde{\psi}_{1,\ldots,N}\rangle$ in Eq. (39), we obtain

$$\tau_{D|\tilde{\psi}_{1,\ldots,N}\rangle} = \frac{1}{N|\alpha|^2(\gamma^+ + \gamma^-)}, \tag{47}$$

which, in the weak coupling limit ($\gamma^{\pm}=\Gamma/N$), reduces exactly to the expected value for the decoherence time of a superposition state $\mathcal{N}_{\pm}(|\alpha\rangle \pm |-\alpha\rangle)$ prepared in a single dissipative oscillator: $(2|\alpha|^2\Gamma)^{-1}$.

Considering the coupling strength $\lambda=2\omega_0/\sqrt{N-1}$ (where the normal mode Ω_1 is shifted to zero and, consequently, $\gamma^- = \gamma/2 = \gamma^+/2 = \Gamma/2N$), we obtain for the decoherence times of the states $|\phi_{1,\ldots,N}\rangle$, $|\tilde{\phi}_{1,\ldots,N}\rangle$, and $|\tilde{\psi}_{1,\ldots,N}\rangle$, respectively,

$$\tau_D|_{|\phi_{1,\ldots,N}\rangle} = \frac{1}{2|\alpha|^2\Gamma}\frac{4}{3N+2\sqrt{N-1}}, \tag{48a}$$

$$\tau_D|_{|\tilde{\phi}_{1,\ldots,N}\rangle} = \frac{1}{2|\alpha|^2\Gamma}\frac{4(N-1)}{8S(N-1)-2\sqrt{N-1}-N}, \tag{48b}$$

$$\tau_D|_{|\tilde{\psi}_{1,\ldots,N}\rangle} = \frac{4}{3}\frac{1}{2|\alpha|^2\Gamma}. \tag{48c}$$

For $N=2$ ($S=1$) the results in both topologies must be exactly the same. In fact, Eqs. (48a)–(48c) reduce, as they should, to those of a symmetric network: $\tau_D|_{|\phi_{1,\ldots,N}\rangle} = (4|\alpha|^2\Gamma)^{-1}$, $\tau_D|_{|\tilde{\phi}_{1,\ldots,N}\rangle} = (2|\alpha|^2\Gamma)^{-1}$, and $\tau_D|_{|\tilde{\psi}_{1,\ldots,N}\rangle} = (4/3) \times (2|\alpha|^2\Gamma)^{-1}$. We note that the decoherence times of the states $|\phi_{1,\ldots,N}\rangle$, $|\tilde{\phi}_{1,\ldots,N}\rangle$, and $|\tilde{\psi}_{1,\ldots,N}\rangle$ for $N>2$, obtained in Eqs. (48a)–(48c), are larger than the equivalent values in a symmetric network. In fact, with the coupling strength $\lambda = 2\omega_0/\sqrt{N-1}$, we have $\gamma^- = \Gamma/2N$ for the central-oscillator network and $\gamma^- = \Gamma/N$ for the symmetric network. Considering now the coupling strength $\lambda = 2\omega_0$, we obtain, for $N>2$, the decoherence times

$$\tau_D|_{|\phi_{1,\ldots,N}\rangle} = \frac{1}{2N|\alpha|^2\Gamma}, \tag{49a}$$

$$\tau_D|_{|\tilde{\phi}_{1,\ldots,N}\rangle} = \frac{1}{4S|\alpha|^2\Gamma}, \tag{49b}$$

$$\tau_D|_{|\tilde{\psi}_{1,\ldots,N}\rangle} = \frac{1}{2|\alpha|^2\Gamma}, \tag{49c}$$

which are smaller than those in Eqs. (48a)–(48c) due to the fact that for $\lambda = 2\omega_0$ the normal mode Ω_1 is not shifted to zero and, consequently, the damping rate γ^- assumes the same values as γ and γ^+, i.e., $\gamma^- = \Gamma/N$. However, the results in Eqs. (49a)–(49c) are exactly the same as those computed for a symmetric network since the cross decay-channels become null in both topologies when $\lambda = 2\omega_0$, with Markovian white noise. We stress that the cross-decay channels are the ingredient which differentiates the coherence dynamics of the two topologies.

We finally note that we can prepare particular states of the network whose decoherence times depend only on γ or even on γ^- (or γ^+). As an example, considering $R-S = \pm\sqrt{N-1}$ the decoherence time depends only on $\gamma^{\pm}$ and γ. Concerning to $N=5$, $R=1$, and $S=3$, such that $R-S = -\sqrt{N-1}$, we get the state $\mathcal{N}(|\alpha,\alpha,-\alpha,-\alpha,-\alpha\rangle \pm |-\alpha,-\alpha,\alpha,\alpha,\alpha\rangle)$ and the decoherence time

$$\tau_D = \frac{1}{10|\alpha|^2(2\gamma^- + 3\gamma)}, \tag{50}$$

which becomes, for Markovian white noise, $(\frac{1}{4})(2|\alpha|^2\Gamma)^{-1}$, whereas, in the symmetric network, we obtain the same result as in the weak-coupling limit: $(\frac{1}{5})(2|\alpha|^2\Gamma)^{-1}$. To broaden our understanding of the above results regarding decoherence times, next we proceed to analyze the recurrence and swap dynamics of quantum states in the central-oscillator network.

VII. STATE RECURRENCE AND SWAP DYNAMICS

Considering the case where all the oscillators in the network have the same damping factor $\Gamma_m = \Gamma$, we analyze in this section the effect of dissipation on two phenomena: the swap of the superposition state $\mathcal{N}_{\pm}(|\alpha\rangle \pm |-\alpha\rangle)_1$, prepared in the central oscillator 1, to one of the peripheral oscillators $\ell = 2,\ldots,N$ coupled to the central one and the subsequent recurrence of this superposition to the central oscillator. Assuming, in the strong-coupling regime, that the central-oscillator network is prepared in the superposition state (39),

$$|\tilde{\psi}_{1,\ldots,N}\rangle = \mathcal{N}_{\pm}(|\alpha\rangle \pm |-\alpha\rangle)_1 \otimes |\{\eta\}_\ell\rangle,$$

we calculate, as for the symmetric network, the probability of the superposition state $\mathcal{N}_{\pm}(|\alpha\rangle \pm |-\alpha\rangle)_1$ swapping to a particular oscillator among the $\ell=2,\ldots,N$ peripheral oscillators and the probability of recurrence of this superposition state to the central oscillator.

As in Part I we do not expect the probability of the state $\mathcal{N}_{\pm}(|\alpha\rangle \pm |-\alpha\rangle)_1$ swapping to a particular oscillator ℓ to reach unity. There are $N-1$ oscillators coupled to oscillator 1 and the superposition $\mathcal{N}_{\pm}(|\alpha\rangle \pm |-\alpha\rangle)_1$ will be pulverized into these oscillators. As we stressed in Part I, this expectation applies only when all couplings are considered to have the same strength λ. In fact, for a central-oscillator network where oscillator 1 couples to the remaining oscillators ℓ with varying strength λ_ℓ, the probability of the superposition $N_{\pm}(|\alpha\rangle \pm |-\alpha\rangle)_1$ swapping into oscillator ℓ will depend on the coupling strength λ_ℓ. Therefore, it may occur that the state swap probability to a particular oscillator among the $\ell=2,\ldots,N$ becomes significant if an appropriate coupling strength is assumed.

As far as the superposition state $|\tilde{\psi}_{1,\ldots,N}\rangle$ is concerned, the reduced density operators for the central oscillator 1 and a particular peripheral oscillator, ℓ, derived from Eq. (36), are given, respectively, by

$$\rho_1(t) = \mathcal{N}_{\pm}^2 \sum_{p,q=1}^{2} (\pm)^{1+\delta_{pq}} \exp[-2|\alpha|^2(1-|\mu_{11}|^2)(1-\delta_{pq}) + \theta_1^{pq}] \times |\xi_1^p\rangle\langle\xi_1^q|, \tag{51}$$

and

$$\rho_\ell(t) = \mathcal{N}_{\pm}^2 \sum_{p,q=1}^{2} (\pm)^{1+\delta_{pq}} \exp[-2|\alpha|^2(1-|\mu_{\ell 1}|^2)(1-\delta_{pq}) + \theta_\ell^{pq}] \times |\xi_\ell^p\rangle\langle\xi_\ell^q|, \tag{52}$$

where

$$\theta_m^{pq}(t) = i2\mathrm{Im}\left(\alpha\beta_1^{*p}\mu_{m1}^*(t)\sum_\ell \mu_{m\ell}(t)\right). \tag{53}$$

We note that the expressions for $\rho_1(t)$, $\rho_\ell(t)$, and $\theta_m^{pq}(t)$ are exactly those for the symmetric network, apart from functions $\mu_{m\ell}(t)$. The same observation applies to the recurrence and state-swap probabilities, obtained from the reduced density operators (51) and (52), respectively, which are given by

$$P_R(t) \equiv \mathrm{Tr}[\rho_1(t)\rho_1(0)] = \sum_{p,q=1}^{2} \mathcal{C}_{pq}^1(t)\langle\xi_1^q|(|\alpha\rangle \pm |-\alpha\rangle)_1(\langle\alpha| \pm \langle-\alpha|)|\xi_1^p\rangle, \tag{54a}$$

$$P_S(t) \equiv \mathrm{Tr}[\rho_\ell(t)\rho_1(0)] = \sum_{p,q=1}^{2} \mathcal{C}_{pq}^\ell(t)\langle\xi_\ell^q|(|\alpha\rangle \pm |-\alpha\rangle)_1(\langle\alpha| \pm \langle-\alpha|)|\xi_\ell^p\rangle \tag{54b}$$

with the coefficients

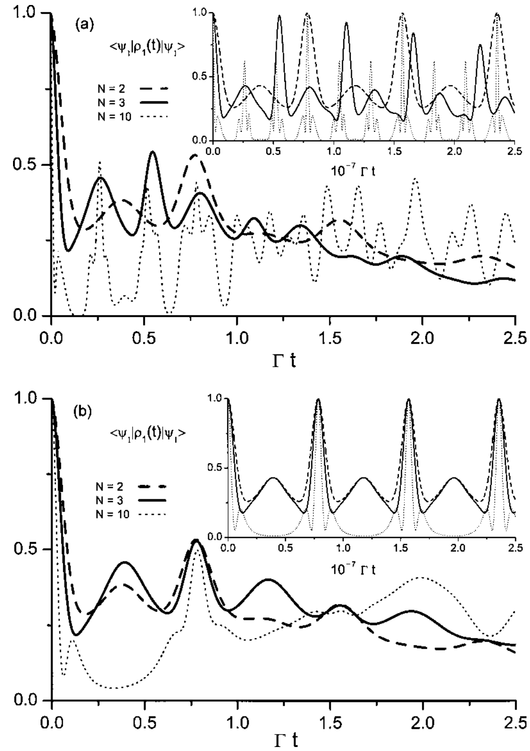

FIG. 2. Recurrence probability $P_R(t)$ plotted against the scaled time Γt, for $\Gamma_m=\Gamma$ (setting fictitious $\Gamma/\omega_0=1/2$) and (a) $\lambda/\omega_0=2$ and (b) $\lambda=2\omega_0/\sqrt{N-1}$, assuming Markovian white noise and the factorized state $|\tilde{\psi}_{1,\ldots,N}\rangle=\mathcal{N}_{\pm}(|\alpha\rangle \pm |-\alpha\rangle)_1 \otimes |\{\eta\}_\ell\rangle$, with real parameters $\alpha=\eta=1$. Curves refer to networks with $N=2,3$, and 10, as indicated. Insets show realistic timescale $\Gamma/\omega_0 \ll 1$ on which $P_R(t)$ returns to near unity many times before perceptible relaxation occurs.

$$\mathcal{C}_{pq}^1(t) = \mathcal{N}_{\pm}^4(\pm)^{1+\delta_{pq}}\exp[-2|\alpha|^2(1-|\mu_{11}|^2)(1-\delta_{pq}) + \theta_1^{pq}], \tag{55a}$$

$$\mathcal{C}_{pq}^\ell(t) = \mathcal{N}_{\pm}^4(\pm)^{1+\delta_{pq}}\exp[-2|\alpha|^2(1-|\mu_{\ell 1}|^2)(1-\delta_{pq}) + \theta_\ell^{pq}]. \tag{55b}$$

In Figs. 2 and 3 we analyze the recurrence and swap probabilities, respectively, assuming Markovian white noise and that all the oscillators have the same damping rate $\Gamma_m=\Gamma$. In order to compare the results from the two topologies, in Figs. 2(a) and 3(a) we plot the recurrence and swap probabilities against the scaled time Γt, employing exactly the parameters adopted in the case of a symmetric network [Figs. 4(a) and 5(a) in Part I of this work]: $\alpha=\eta=1$ as real parameters, $\lambda/\omega_0=2$, and setting the fictitious ratio $\Gamma/\omega_0=1/2$ to show clearly the dissipative dynamics. In Figs. 2(b) and 3(b) we employ these same parameters except for the coupling strength $\lambda=2\omega_0/\sqrt{N-1}$, which shifts the normal mode Ω_1 to zero.

The curves in Fig. 2(a) relate to the values $N=2,3$, and 10, represented by dashed, solid, and dotted lines, respectively. We observe that the recurrence probability $P_R(t)$ decays exponentially due to the dissipative process and, as in the case of the symmetric network, the decay is slower for

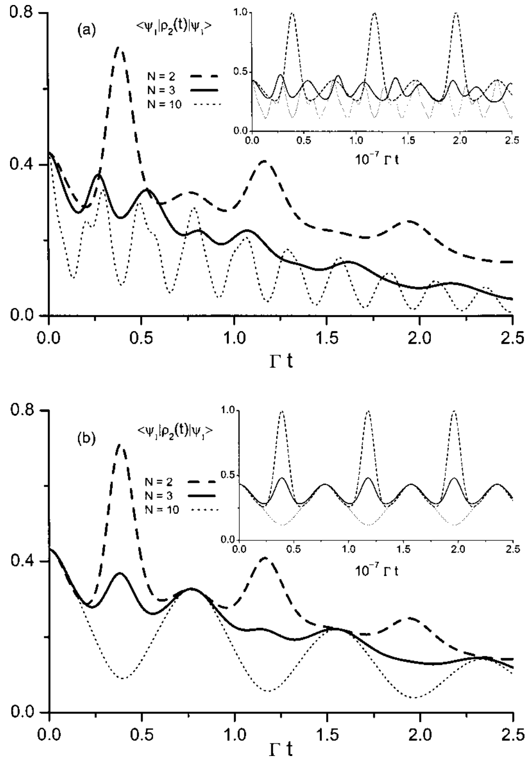

FIG. 3. State-swap probability $P_S(t)$ plotted against the scaled time Γt, for $\Gamma_m = \Gamma$ (setting fictitious $\Gamma/\omega_0 = 1/2$) and (a) $\lambda/\omega_0 = 2$ and (b) $\lambda = 2\omega_0/\sqrt{N-1}$, assuming Markovian white noise and the factorized state $|\tilde{\psi}_{1,\ldots,N}\rangle = \mathcal{N}_{\pm}(|\alpha\rangle \pm |-\alpha\rangle)_1 \otimes |\{\eta\}_{\ell}\rangle$, with real parameters $\alpha = \eta = 1$. Curves refer to networks with $N=2,3$, and 10, as indicated. Insets show realistic timescale $\Gamma/\omega_0 \ll 1$ on which $P_S(t)$ returns to near unity many times before perceptible relaxation occurs.

the case $N=2$ where $\gamma^- = \gamma/2 = \gamma^+/2$. For $N>2$, where $\gamma^- = \gamma = \gamma^+$, the decay of the probability $P_R(t)$ is approximately the same whatever the number of oscillators composing the network. The difference in the results for the two topologies becomes clear when computing the recurrence time [from function $\mu_{11}(t)$ in Eq. (34)] which, for the central-oscillator network, is derived from the relation $\cos(N\lambda t)\cos(\sqrt{N-1}\lambda t) = 1$, giving

$$t_R = \frac{r\pi}{\sqrt{N-1}\lambda} = \frac{s\pi}{N\lambda}, \tag{56}$$

where r and s are integers both even or odd. Therefore, differently from the case of a symmetric network, where the recurrence times get smaller as the number of oscillators in the network rises, for the central-oscillator network the recurrence times follow from a phase-matching between the shifted natural frequency $\tilde{\omega}_0 = N\lambda$ and the coupling $\sqrt{N-1}\lambda$. As shown in the inset, on a realistic scale where $\Gamma/\omega_0 \ll 1$, the probability $P_R(t)$ reaches significant values (around 0.5) many times before the relaxation takes place. These *secondary* recurrences, where the probability assumes significant values, do not appear in the symmetric network and were not considered for computing the recurrence times in Eq. (56).

In Fig. 2(b), concerning the recurrence probability when $\lambda = 2\omega_0/\sqrt{N-1}$, we note on the realistic scale of the inset that the recurrence times turn out the same regardless of the number of oscillators composing the network, being given by

$$t_R = \frac{r\pi}{2\omega_0}, \quad r = 0,1,2,\ldots. \tag{57}$$

In fact, with $\lambda = 2\omega_0/\sqrt{N-1}$ we obtain $\tilde{\omega}_0 = 2\omega_0$ [see Eq. (2)] and, consequently, $\cos(\tilde{\omega}_0 t)\cos(\sqrt{N-1}\lambda t) = \cos^2(2\omega_0 t) = 1$. We note that the curves for $N=2$ in both Figs. 2(a) and 2(b) are exactly the same as expected.

In Fig. 3(a) we analyze the state swap probabilities $P_S(t)$, considering the curves for $N=2,3$, and 10, represented by dashed, solid, and dotted lines, respectively. Evidently, for $N=2$ the superposition $\mathcal{N}_{\pm}(|\alpha\rangle \pm |-\alpha\rangle)_1$ swaps to the oscillator $\ell=2$ as indicated on the realistic scale $(\Gamma/\omega_0 \ll 1)$ in the inset. The probability $P_S(t)$ decays from unity due to the damping process as shown by the dashed line. For $N>2$ we do not obtain a significant value for the swap probability $P_S(t)$, as expected: the superposition state $\mathcal{N}_{\pm}(|\alpha\rangle \pm |-\alpha\rangle)_1$ is pulverized into the $\ell>2$ oscillators connected to oscillator 1. However, in the present case of a central-oscillator network, the state of the network at the "swap times" (assumed to be $t_R/2$) is not an entanglement of the whole system as in the symmetric network. By considering the initial state $|\tilde{\psi}_{1,\ldots,N}\rangle$ and substituting the "swap times" into Eq. (34) it can be derived that the state of the central oscillator (a coherent state ς) decouples from the entanglement between the remaining ℓ oscillators. Therefore, at the "swap times" we obtain

$$|\psi_{swap}\rangle = \mathcal{N}|\varsigma_1\rangle \otimes (|\{\varepsilon_{\ell}\}\rangle + |\{-\varepsilon_{\ell}\}\rangle), \tag{58}$$

where $\varsigma_1 = -\eta/\sqrt{N-1}$ and $\varepsilon_{\ell} = \varepsilon = \alpha/\sqrt{N-1}$. Thus, the state of the whole system oscillates between $|\tilde{\psi}_{1,\ldots,N}\rangle$ (where the central oscillator is in a "Schrödinger cat"-like state and the remaining oscillators in coherent states $|\eta\rangle$) and $|\psi_{swap}\rangle$ [where the central oscillator is a coherent state $|\varsigma\rangle$ and the remaining oscillators are entangled as in Eq. (58)]. The state in Eq. (58) shows how the "Schrödinger cat"-like state, initially prepared in oscillator 1, is pulverized into the $N-1$ oscillators of the network.

Finally, in Fig. 3(b) we plot the curves for the swap probabilities considering $\lambda = 2\omega_0/\sqrt{N-1}$. As in Fig. 3(a) the swap of the superposition $\mathcal{N}_{\pm}(|\alpha\rangle \pm |-\alpha\rangle)_1$ to the remaining $N-1$ oscillators occurs only when $N=2$. We next analyze the linear entropies of the whole system, the central-oscillator, and the $N-1$ oscillators coupled to the central one.

VIII. ENTROPY EXCESS

Considering again the state $|\tilde{\psi}_{1,\ldots,N}\rangle = \mathcal{N}_{\pm}(|\alpha\rangle \pm |-\alpha\rangle)_1 \otimes |\{\eta_{\ell}\}\rangle$, a Markovian white noise reservoir, and the case where all the oscillators in the network have the same damping factor $\Gamma_m = \Gamma$, in this section we analyze the linear entropies for the joint state, the reduced state of oscillator 1, and the reduced state of all the remaining $N-1$ oscillators. These functions, computed from Eqs. (40), (51), and (52), are given, respectively, by

$$\mathcal{S}_{1,\ldots,N}(t) = 1 - \mathrm{Tr}_{1,\ldots,N}\rho_{1,\ldots,N}^2(t), \tag{59a}$$

$$\mathcal{S}_1(t) = 1 - \mathrm{Tr}_1\rho_1^2(t), \tag{59b}$$

$$\mathcal{S}_{2,\ldots,N}(t) = 1 - \mathrm{Tr}_{2,\ldots,N}[\mathrm{Tr}_1\rho_{1,\ldots,N}(t)]^2. \tag{59c}$$

The evolution of the correlation between the reduced states of oscillator 1 and all the remaining $N-1$ oscillators will be analyzed through the excess entropy defined as

$$\mathcal{E} \equiv \mathcal{S}_1 + \mathcal{S}_{2,\ldots,N} - \mathcal{S}_{1,\ldots,N}. \tag{60}$$

In Fig. 4 the quantities in Eqs. (59a)–(59c) and (60) are plotted against the scaled time Γt, considering $\alpha=\eta=1$ as real parameters, setting the fictitious ratio $\lambda/\Gamma=4$ (to display the dissipative dynamics more clearly) and the coupling strength $\lambda=2\omega_0$. Figures 4(a)–4(d) refer to $N=2,3,10$, and 50, respectively. In these figures, as in the symmetric network, the thick solid line representing the linear entropy of the joint state $\mathcal{S}_{1,\ldots,N}$, starts from zero, goes to a maximum due to the decoherence process (or the entanglement between the whole system composed of the oscillators of the network and their respective reservoirs), and then returns to zero, since in the asymptotic limit all oscillators reach the vacuum for a reservoir at absolute zero. Meanwhile, the linear entropies of the reduced states $\mathcal{S}_1$ and $\mathcal{S}_{2,\ldots,N}$, represented by solid and dashed lines, respectively, oscillate between 0 and 0.5. The case $N=2$ coincides, as expected, with that of a symmetric network, where the "Schrödinger cat"-like state prepared in oscillator 1 swaps to oscillator 2 and recurs, subsequently, to oscillator 1. In fact, the function $\mathcal{S}_1$ ($\mathcal{S}_2$) reach its minima as oscillator 1 (oscillator 2) assumes (recovers) the state $|-\eta\rangle_1$ ($|\eta\rangle_2$), as can be computed from Eq. (34) [1]. At the same time, $\mathcal{S}_2$ ($\mathcal{S}_1$) touches the thick solid line representing $\mathcal{S}_{1,2}$, from above, indicating that the superposition $\mathcal{N}_\pm(|\alpha\rangle\pm|-\alpha\rangle)_1$ has swapped (recurred) to oscillator 2(1) on its way to decoherence. We conclude that it is exactly the state $\mathcal{N}_\pm(|\alpha\rangle\pm|-\alpha\rangle)_1$ which recurs (swaps) to oscillator 1(2), from Figs. 2 and 3, concerned with the recurrence and swap probabilities, respectively, which show that this superposition does recur and swap to oscillator 1(2), on its way to decoherence.

From Fig. 4 we also observe that the maximal correlations between the central oscillator 1 and the peripheral ones occur at the points where the curves $\mathcal{S}_1$ and $\mathcal{S}_{2,\ldots,N}$ cross each other, as illustrated by the dotted line representing the excess entropy $\mathcal{E}$. When the linear entropy $\mathcal{S}_1$ ($\mathcal{S}_{2,\ldots,N}$) touches the curve $\mathcal{S}_{1,\ldots,N}$, i.e., when the superposition state $\mathcal{N}_\pm(|\alpha\rangle\pm|-\alpha\rangle)_1$ recurs to oscillator 1 (and the remaining $N-1$ oscillators get into the entanglement $\mathcal{N}(|\{\varepsilon_\ell\}\rangle+|\{-\varepsilon_\ell\}\rangle)$, as in Eq. (58)), both the excess entropy and the correlation between the oscillators reach their minima. We observe that in the "swap times" $t_R/2$, where $\rho_1(t_R/2)=|s_1\rangle\langle s_1|$ and $\rho_{2,\ldots,N}(t_R/2)=\mathcal{N}^2(|\{\varepsilon_\ell\}\rangle+|\{-\varepsilon_\ell\}\rangle)(\langle\{\varepsilon_\ell\}|+\langle\{-\varepsilon_\ell\}|)$, we obtain

$$\begin{aligned}\mathcal{S}_{1,\ldots,N}(t_R/2) &= 1 - \mathrm{Tr}_1\rho_1^2(t_R/2)\mathrm{Tr}_{2,\ldots,N}\rho_{2,\ldots,N}^2(t_R/2)\\ &= 1 - \mathrm{Tr}_{2,\ldots,N}\rho_{2,\ldots,N}^2(t_R/2) = \mathcal{S}_{2,\ldots,N}(t_R/2).\end{aligned} \tag{61}$$

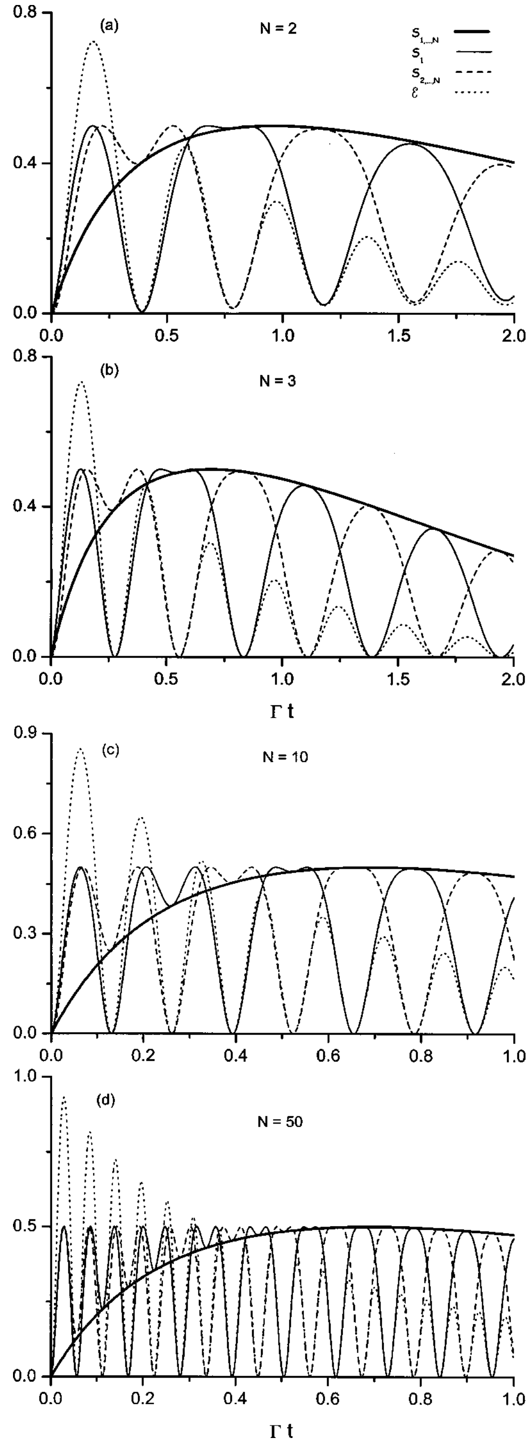

FIG. 4. Linear entropies $\mathcal{S}_{1,\ldots,N}(t)$ (thick solid line), $\mathcal{S}_1(t)$ (solid line), $\mathcal{S}_{2,\ldots,N}(t)$ (dashed line), and excess entropy $\mathcal{E}$ (dotted line) plotted against Γt, for $\Gamma_m=\Gamma$ (setting fictitious $\lambda/\Gamma=4$) and $\lambda=2\omega_0$, assuming Markovian white noise and the factorized state $|\tilde{\psi}_{1,\ldots,N}\rangle=\mathcal{N}_\pm(|\alpha\rangle\pm|-\alpha\rangle)_1\otimes|\{\eta\}_\ell\rangle$, with real parameters $\alpha=\eta=1$. Networks with (a) $N=2$, (b) $N=3$, (c) $N=10$, and (d) $N=50$.

We note that, as time goes on, the oscillators do not get completely disentangled for the case $N=2$ since the excess entropy does not reach zero. This occurs since, for $N=2$, $\gamma^+=2\gamma^-=\Gamma/2$ and, consequently, the cross-decay channel $\mathcal{L}_{12}\rho_{12}$ is not null, leading to the development of a background correlation which gets both oscillators permanently entangled. When $N>2$ we obtain the same value for the split decay rates $\gamma^{\pm}=\Gamma/N$ and, thus, the cross-decay channel is null, preventing the development of the background correlation. As observed in Part I of this work, the background correlation arises from two different processes: (i) the cross-decay channels $[\mathcal{L}_{\ell n}\rho_{1,\ldots,N}(t)]$ which link together the individual Liouville operators $\mathcal{L}_m\rho_{1,\ldots,N}(t)$ and (ii) the usual decay channels $[\mathcal{L}_m\rho_{1,\ldots,N}(t)]$ when the decay rates Γ_m are different from each other. For equal decay rates, as occurring here when $N>2$, the individual decay channels do not contribute to the development of the background correlation.

The essential difference between the curves in Fig. 4 for the central-oscillator network and those for the symmetric network (Fig. 6 in Part I) is that in the symmetric network the remaining $N-1$ oscillators act as part of the reservoir for oscillator 1 where the "Schrödinger cat"-like state $\mathcal{N}_{\pm}(|\alpha\rangle\pm|-\alpha\rangle)_1$ is prepared. As N increases, the "Schrödinger cat"-like state hardly leaves oscillator 1 since the recurrence time becomes smaller as N increases [see Eq. (70) in Part I]. Therefore, in a symmetric network with $N\gg 1$, the "Schrödinger cat"-like state prepared in oscillator 1 behaves as if this oscillator is decoupled from the remaining $N-1$ oscillators composing the network. Differently from the case of a symmetric network, in the central-oscillator network, the remaining $N-1$ oscillators do not act as part of the reservoir for the central oscillator 1. Instead, as described above, the state of the whole system oscillates between $|\tilde{\psi}_{1,\ldots,N}\rangle$ and $|\psi_{swap}\rangle$, i.e., the "Schrödinger cat"-like state prepared in oscillator 1 is pulverized to the remaining oscillators in the network, as in the symmetric network, but in a way that the peripheral oscillators get into the coherent superposition $\mathcal{N}[|\{\varepsilon_\ell\}\rangle+|\{-\varepsilon_\ell\}\rangle]$ with decouples from the state of oscillator 1 in the "swap times."

Concerning the possibility of protecting the superposition state $\mathcal{N}_{\pm}(|\alpha\rangle\pm|-\alpha\rangle)_1$, prepared in oscillator 1, by coupling it to the peripheral oscillators to obtain the decoherence times $\tau_D|_{|\tilde{\psi}_{1,\ldots,N}\rangle}=(4/3)(2|\alpha|^2\Gamma)^{-1}$, we note that the background correlation developed in Fig. 4(a) does not affect significantly the fidelity of the recovered superposition $\mathcal{N}_{\pm}(|\alpha\rangle\pm|-\alpha\rangle)_1$. The correlation time, estimated as the time when the minima of $\mathcal{E}$ approach 10^{-2}, is written as

$$\tau_C \approx \frac{0.1}{|\alpha|}\frac{1}{|\gamma^+-\gamma^-|}. \tag{62}$$

In the weak-coupling regime, where $\gamma^+=\gamma^-=\Gamma/N$, the background-correlation time goes to infinity, so that the entropy $\mathcal{S}_{2,\ldots,N}$ always returns to zero in the recurrence time. Considering the decoherence time τ_D computed in the strong coupling regime [Eq. (47)], we obtain the ratio τ_C/τ_D

$$\frac{\tau_C}{\tau_D} \approx \frac{N|\alpha|}{10}\frac{\gamma^++\gamma^-}{|\gamma^+-\gamma^-|}. \tag{63}$$

For $\tau_C/\tau_D\gtrsim 1$ the correlation time becomes greater than the decoherence time, and thus becomes negligible for state protection purposes. Assuming Markovian white noise we obtain the ratio $\tau_C/\tau_D\to\infty$ for $N>2$ as expected from the curves in Figs. 4(b)–4(d). However, for $N=2$ we obtain the same result as in Part I, where $\tau_C/\tau_D=3|\alpha|/5$ so that, for $|\alpha|\gtrsim 2$ we obtain $\tau_C/\tau_D\gtrsim 1$. As stressed in Part I, this mechanism for state protection could be employed in cavity quantum electrodynamics, where a superposition state $\mathcal{N}_{\pm}(|\alpha\rangle\pm|-\alpha\rangle)_1$ could be prepared in an open "bad-quality" cavity, protected against decoherence in a system of closed "good-quality" cavities and be rescued back in the open cavity, say, for atom-field interaction purposes.

Finally, we note that for the coupling strength $\lambda=2\omega_0/\sqrt{N-1}$ we obtain exactly the curves in Fig. 4(a), whatever the value N. In fact, it is readily shown that the oscillations of the linear entropies $\mathcal{S}_1(t)$ and $\mathcal{S}_{2,\ldots,N}(t)$, as well as the excess entropy $\mathcal{E}$, arise from $\cos(\sqrt{N-1}\lambda t)$ and, consequently, with $\lambda=2\omega_0/\sqrt{N-1}$ we obtain $\cos(2\omega_0 t)$, which is independent on N.

IX. CONCLUSION

In this paper we investigated the coherence dynamics and the decoherence process of quantum states in a network composed of N coupled dissipative oscillators. We have considered a central-oscillator network where a central dissipative oscillator is assumed to interact with $N-1$ peripheral noninteracting dissipative oscillators. The results obtained for this topology were compared with those in Part I of this paper, where a symmetric topology was considered, i.e., a network of N oscillators, each interacting with all the others. As in Part I, assuming all oscillators to have the same natural frequency ω_0 and all couplings the same strength λ, we considered both regimes of weak and strong couplings between the oscillators. We have referred to the regime as strong-coupling in the situations where the parameter $\lambda\sqrt{N-1}$ is large enough to shift the normal modes to regions far from the natural frequency ω_0. These situations arise when the coupling strength between the oscillators and/or the number of oscillators in the network are increased.

As first stressed in Ref. [1] (where an exhaustive analysis of a network composed of only two oscillators was developed) and in Part I of this work, the essential feature of strong coupling between the oscillators is to shift the normal-mode frequencies to regions far from the system natural frequency ω_0. Therefore, if the spectral densities of the reservoirs around the normal-mode frequencies are significantly different from that around ω_0, the coherence dynamics of the system may be significantly modified. In this way, for a network of strongly coupled systems the spectral densities of the reservoirs play a crucial role in the dissipative dynamics and, consequently, the program of quantum-reservoir engineering.

Instead of the two normal modes derived for the symmetric network, $\Omega_1=\tilde{\omega}_0+(N-1)\lambda$ and $\Omega_\ell=\tilde{\omega}_0-\lambda$, the central-oscillator network displays three different normal modes $\Omega_1=\tilde{\omega}_0-\lambda\sqrt{N-1}$, $\Omega_j=\tilde{\omega}_0$ $(j=2,\ldots,N)$, and $\Omega_N=\tilde{\omega}_0+\lambda\sqrt{N-1}$. Moreover, when considering the coupling strength $\lambda=2\omega_0/\sqrt{N-1}$, the normal mode Ω_1 is shifted to zero for any number N of oscillators in the network. This is a crucial difference between the symmetric and the central-oscillator networks, since in the former, one of the normal modes, $\Omega_1=\tilde{\omega}_0-\lambda$, is shifted to zero only for the particular case $N=2$. Therefore, even for a markovian white noise reservoir, the decoherence time of quantum superposition states is increased when a central-oscillator network is adopted, whatever the value of N. As the normal mode $\Omega_1=\tilde{\omega}_0-\lambda\sqrt{N-1}$ is shifted to zero, the coupling between the oscillators and their respective reservoirs becomes half the original and, thus, the decoherence time increases.

As we have concluded in Part I, when considering states of the network which are eigenstates of the normal modes Ω_1 and Ω_ℓ, i.e., eigenstates of the frequencies shifted to regions far away from the natural frequency ω_0, their decoherence times may be significantly improved, depending on the spectral density of the reservoirs. For a reservoir whose spectral density is given by the Bose–Einstein distribution [22,23], for example, the decoherence time of an eigenstate of the normal mode Ω_1 is increased due to the exponential decay of the spectral density. For the central-oscillator network analyzed in this paper, we could not obtain the eigenstate associated with the normal modes. This task is more difficult for the central-oscillator network, due to its lack of complete symmetry.

We also stress that for the case $N=2$, where both topologies coincide, the decoherence time of the state $\mathcal{N}_\pm(|\alpha\rangle \pm|-\alpha\rangle)_1\otimes|\eta_2\rangle$, a "Schrödinger-cat"-like state prepared in oscillator 1 and a coherent state prepared in oscillator 2, increases by a factor $\frac{8}{3}$ when considering distinct damping factors, such that $\Gamma_1\gg\Gamma_2$, Markovian white noise, and the strong-coupling regime. Even in the weak-coupling regime with Markovian white noise, the decoherence time increases by the factor 2 when $\Gamma_1\gg\Gamma_2$. For an arbitrary N and considering the state $|\tilde{\psi}_{1,\dots,N}\rangle=\mathcal{N}_\pm(|\alpha\rangle\pm|-\alpha\rangle)_1\otimes|\{\eta_\ell\}\rangle$ (where a "Schrödinger-cat"-like state is prepared in oscillator 1 while all the other oscillators are prepared in the coherent states η), the decoherence time of the superposition $\mathcal{N}_\pm(|\alpha\rangle\pm|-\alpha\rangle)_1$ increases, even for Markovian white noise, when assuming $\Gamma_1\gg\Gamma_2$, in both topologies. This result was verified for the symmetric network and must hold also for the central-oscillator network, where just the case $\Gamma_1=\Gamma_2$ was computed (owing to analytical difficulties). However, when $N\gg1$ the remaining $N-1$ oscillators of the symmetric network behave as if they were part of the reservoir and the decoherence time of the superposition $\mathcal{N}_\pm(|\alpha\rangle\pm|-\alpha\rangle)_1$ remains unchanged in both cases $\Gamma_1\neq\Gamma_2$ and $\Gamma_1=\Gamma_2$. However, for the central-oscillator network, with $\Gamma_1=\Gamma_2$, the decoherence time of the state $|\tilde{\psi}_{1,\dots,N}\rangle=\mathcal{N}_\pm(|\alpha\rangle\pm|-\alpha\rangle)_1\otimes|\{\eta_\ell\}\rangle$ is always increased by the factor $\frac{4}{3}$ for any value of N, when considering the coupling strength $\lambda=2\omega_0/\sqrt{N-1}$, which shifts Ω_1 to zero. This result follows from the swap dynamics discussed below.

Analyzing the state swap and recurrence dynamics, we started once more from the state $|\tilde{\psi}_{1,\dots,N}\rangle=\mathcal{N}_\pm(|\alpha\rangle\pm|-\alpha\rangle)_1\otimes|\{\eta_\ell\}\rangle$ and verified that for the central-oscillator network the state of the whole system oscillates between $|\tilde{\psi}_{1,\dots,N}\rangle$ and $|\psi_{swap}\rangle=\mathcal{N}|\varsigma_1\rangle\otimes(|\{\varepsilon_\ell\}\rangle+|\{-\varepsilon_\ell\}\rangle)$ (where the central oscillator is a coherent state $|\varsigma\rangle$ while all the peripheral oscillators are entangled). At the recurrence times the network returns to the state $|\tilde{\psi}_{1,\dots,N}\rangle$ while at the "swap times" (assumed to be half-way between the recurrence times) it is the product defined by $|\psi_{swap}\rangle$. In fact, there is not a swap of the initial superposition state $\mathcal{N}_\pm(|\alpha\rangle\pm|-\alpha\rangle)_1$ prepared in oscillator 1 to the peripheral oscillators. The state $|\psi_{swap}\rangle$) shows how this "Schrödinger-cat"-like state is pulverized into the $N-1$ oscillators of the network. That is why we used the term "swap times." In the symmetric network, where each oscillator is coupled to each other, starting with the state $|\tilde{\psi}_{1,\dots,N}\rangle$ we obtain in the "swap times" an entanglement of the whole system, instead of the product expressed by $|\psi_{swap}\rangle$.

From the above we conclude that the topology defines the coherence dynamics and decoherence times of quantum states of the network. However, such phenomena depend crucially on the state of the network. As pointed out above, in the strong-coupling regime the spectral densities of the reservoir associated with each oscillator of the network play a decisive role in the coherence dynamics and decoherence process.

We stress that a great amount of work can be done starting with the present analyses of coherence dynamics in a network. First of all we note that (i) it is interesting to consider different coupling strengths between the oscillators. This problem can be solved analytically for a network comprising three oscillators. Certainly, a lot of information concerning the coherence dynamics of particular quantum states of the network can be extracted from this system. Moreover, numerical simulations can be employed to investigate a network with an arbitrary number of oscillators coupled to each other with different strengths. We also stress that, in this case of different coupling strengths between the oscillators, the swap process may be completely different. In fact, a "Schrödinger-cat"-like state $\mathcal{N}_\pm(|\alpha\rangle\pm|-\alpha\rangle)_1$ initially prepared in oscillator 1 could show a high probability of swapping to a given oscillator coupled to oscillator 1 with a strength higher than those of the others.

(ii) We also note that we have not computed correlation functions between the oscillators of the network and the dependence of these correlations on the topology. Such a calculation would be interesting to show, for example in the central-oscillator network, how the peripheral oscillators interact with each other through the central one. How the topology influences particular correlation functions involving, for example, the quadrature operators $\langle X_\ell^1(t)X_{\ell'}^1(t')\rangle$, $\langle X_\ell^2(t)X_{\ell'}^2(t')\rangle$, and $\langle X_\ell^1(t)X_{\ell'}^2(t')\rangle$, where the subscripts label the oscillators and the superscript labels the quadratures 1 and 2. Evidently, other correlation functions can be defined.

(iii) A useful analysis to be done is the coherence dynamics and decoherence times of the state $(|0\rangle\pm|1\rangle)_1\otimes|\{0_\ell\}\rangle$ where a quantum bit is prepared in oscillator 1 while all the other oscillators are in the vacuum state. In addition, we can consider the initial state where all the oscillators of the network are prepared as a quantum bit $|0\rangle\pm|1\rangle$. This particular state could simulate closely the coherence dynamics in a logical processor.

Finally we mention that the present work, enlarging perspectives for coherence dynamics in quantum networks, might provide a motivation for future theoretical and experimental investigations. Together with other works on the decoherence process in an *N*-dimensional quantum system [24], optimization [25], separability of mixed states, and transmission [14,15] in quantum networks [26], it provides a first step in the understanding of a large-scale quantum logic processor.

ACKNOWLEDGMENTS

We wish to express thanks for the support from the Brazilian agencies FAPESP (under Contract Nos. 99/11859-3, 00/15084-5, and 02/02633-6) and CNPq (Intituto do Milênio de Informação Quântica). We also thank R. M. Serra, C. J. Villas-Bôas, P. S. Pizani, V. V. Dodonov, S. S. Mizrahi, and A. F. R. de Toledo Piza for helpful discussions.

[1] M. A. de Ponte, M.C. de Oliveira, and M. H. Y. Moussa, e-print quant-ph/0309082.

[2] S. G. Mokarzel, A. N. Salgueiro, and M. C. Nemes, Phys. Rev. A **65**, 044101 (2002).

[3] H. Zoubi, M. Orenstien, and A. Ron, Phys. Rev. A **62**, 033801 (2000).

[4] J. M. Raimond, M. Brune, and S. Haroche, Phys. Rev. Lett. **79**, 1964 (1997).

[5] C. Monroe, D. M. Meekhof, B. E. King, W. M. Itano, and D. J. Wineland, Phys. Rev. Lett. **75**, 4714 (1995).

[6] L. M. K. Vandersypen, M. Steffen, G. Breyta, C. S. Yannoni, M. H. Sherwood, and I. L. Chuang, Nature (London) **414**, 883 (2001).

[7] S. Haroche, Philos. Trans. R. Soc. London, Ser. A **361**, 1339 (2003).

[8] J. F. Poyatos, J. I. Cirac, and P. Zoller, Phys. Rev. Lett. **77**, 4728 (1996).

[9] C. J. Myatt, B. E. King, Q. A. Turchette, C. A. Sackett, D. Kielpinski, W. M. Itano, C. Monroe, and D. J. Wineland, Nature (London) **403**, 269 (2000).

[10] A. R. R. Carvalho, P. Milman, R. L. de Matos Filho, and L. Davidovich, Phys. Rev. Lett. **86**, 4988 (2001).

[11] N. Lutkenhaus, J. I. Cirac, and P. Zoller, Phys. Rev. A **57**, 548 (1998).

[12] L. M. K. Vandersypen, M. Steffen, G. Breyta, C. S. Yannoni, M. H. Sherwood, and I. L. Chuang, Nature (London) **414**, 883 (2001).

[13] T. Pellizzari, Phys. Rev. Lett. **79**, 5242 (1997); H. J. Briegel, W. Dür, J. I. Cirac, and P. Zoller, *ibid.* **81**, 5932 (1998).

[14] J. I. Cirac, P. Zoller, H. J. Kimble, and H. Mabuchi, Phys. Rev. Lett. **78**, 3221 (1997).

[15] S. van Enk, J. I. Cirac, P. Zoller, H. J. Kimble, and H. Mabuchi, Fortschr. Phys. **46**, 689 (1998).

[16] B. Yurke and J. S. Denker, Phys. Rev. A **29**, 1419 (1984).

[17] A. M. Wang, Chin. Phys. Lett. **18**, 166 (2001); **19**, 620 (2002).

[18] S. L. Zhu, Z. D. Wang, and K. Yang, Phys. Rev. A **68**, 034303 (2003).

[19] G. Mahler and I. Kim, Lect. Notes Comput. Sci. **1509**, 89 (1999).

[20] G. W. Ford, J. T. Lewis, and R. F. O'Connell, Phys. Rev. A **37**, 4419 (1988); G. W. Ford and R. F. O'Connell, Physica A **37**, 377 (1997).

[21] M. Rosenau da Costa, A. O. Caldeira, S. M. Dutra, and H. Westfahl, Jr., Phys. Rev. A **61**, 022107 (2000).

[22] E. Joos and H. D. Zeh, Z. Phys. B: Condens. Matter **59**, 223 (1985).

[23] M. C. de Oliveira, N. G. Almeida, S. S. Mizrahi, and M. H. Y. Moussa, Phys. Rev. A **62**, 012108 (2000).

[24] G. Teklemariam, E. M. Fortunato, C. C. Lopez, J. Emerson, J. Pablo Paz, T. F. Havel, and D. G. Cory, Phys. Rev. A **67**, 062316 (2003).

[25] A. Blais, Phys. Rev. A **64**, 022312 (2001).

[26] Z. Y. Gu and S. W. Qian, Commun. Theor. Phys. **40**, 151 (2003).